A study of two-electron quantum dot spectrum using discrete variable representation method

Frederico V. Prudente, Luis S. Costa, and José David M. Vianna

A study of two-electron quantum dot spectrum using discrete variable representation method

Frederico V. Prudente[a)]
Instituto de Física, Universidade Federal da Bahia 40210-340 Salvador-BA, Brazil

Luis S. Costa[b)]
Instituto de Física, Universidade de Brasília, 70910-900 Brasília DF, Brazil

José David M. Vianna[c)]
Instituto de Física, Universidade Federal da Bahia 40210-340 Salvador BA, Brazil and Instituto de Física, Universidade de Brasília, 70910-900 Brasilia DF, Brazil

A variational method called discrete variable representation is applied to study the energy spectra of two interacting electrons in a quantum dot with a three-dimensional anisotropic harmonic confinement potential. This method, applied originally to problems in molecular physics and theoretical chemistry, is here used to solve the eigenvalue equation to relative motion between the electrons. The two-electron quantum dot spectrum is determined then with a precision of at least six digits. Moreover, the electron correlation energies for various potential confinement parameters are investigated for singlet and triplet states. When possible, the present results are compared with the available theoretical values. © *2005 American Institute of Physics*. [DOI: 10.1063/1.2131068]

I. INTRODUCTION

The study of confined quantum systems has been the subject of investigation of physicists and theoretical chemists since the beginning of quantum theory. In 1928, Fock[1] studied an electron confined by a harmonic oscillator potential in a uniform magnetic field. This problem was investigated by Darwin[2] two years later, obtaining some more properties. Michels *et al.*[3] proposed in 1937 the model of a hydrogen atom in a spherical cage to simulate the effect of pressure on an atom. They were soon followed by Sommerfeld and Welker[4] who recognized the importance of the model of a compressed atom for astrophysics. Meanwhile, Schrödinger[5] studied the case of an atom confined by a cotangent potential. Since then, problems concerning confined quantum systems have been studied by many authors (see Refs. 6–8 for a partial listing of references in this field).

The interest in the study of the physical properties of confined quantum systems has increased with the recent advances of experimental techniques used in mesoscopic-scale semiconductor structures.[9,10] They have allowed the construction of new quantum systems as artificial atoms and molecules[11,12] or quantum dots[13,14] where the number of confined electrons can be controlled. Moreover, the study of the confined systems is also important in catalysis when adsorption phenomena are investigated[15] in the embedding of atoms and molecules inside cavities such as zeolite molecular sieves,[16] fullerenes,[17–20] or solvent environments[21] and in bubbles formed around foreign objects in the liquid helium or neutral plasma,[22–24] for instance. Also, one can study confined phonons,[25] polaritons and plasmons,[26] and confined bosonic gases.[27]

One of the first nontrivial confined quantum systems that shows the interplay of electron-electron interaction and spin effects is the two-electron quantum dot; it is also an interesting candidate to be a qubit in quantum computation.[28,29] The properties of the two-electron quantum dot are dependent on many different issues such as the way to simulate the spatial confinement and its geometric shape, the presence and the position of impurities, the existence of external electrical and/or magnetic field, and the inclusion of many-body effects.

Traditionally, the spatial confinement of a quantum system can be simulated by the imposition of the boundary conditions on the wave functions,[30–34] by changing the actual potential to a model one,[35] and by the introduction of a confinement potential;[36,37] some of these are employed to treat quantum dot systems. On the other hand, several geometric kinds are used as the confining potential in a quantum dot. Maybe the most common quantum dot with two interacting electrons is the two-dimensional isotropic harmonic potential.[38–41] However, many other models have been used, such as the spherical box with finite[42] and infinite[43–46] walls, the two-dimensional harmonic potential with anharmonic correction,[47] the one-dimensional,[48] square[49,50] and cubic[51,52] boxes with infinite walls, the ellipsoidal quantum dot,[53] the Gaussian confining potential,[54] the two-dimensional anisotropic harmonic potential,[55] and the three-dimensional isotropic[56–60] and anisotropic[61,62] potentials.

Other indispensable ingredients to a precise determination of quantum effects in the two-electron quantum dots are the accuracy of the description of electron-electron interaction and the quality of the calculation. Various theoretical

[a)]Electronic mail: prudente@ufba.br
[b)]Electronic mail: luis@fis.unb.br
[c)]Electronic mail: david@ufba.br

approaches have been used for this purpose. We can cite, among them, the Hartree approximation,[63,64] the Hartree-Fock procedure,[33,42,46,63,65,66] the configuration interaction (CI) method,[32,44,46,49] the density-functional theory,[45,50,58,65,67] the exact diagonalization,[51,68] the Green function,[69] the quantum Monte Carlo technique,[70,71] the analytical approaches,[56,72,73] the algebraic procedure,[74] the perturbation theory,[53] the WKB treatment,[75] and the random-phase approximation.[76] Most of these studies are limited to ground-state and few excited-state properties.[61,77] Due to the number of studies, the two-electron quantum dot is an attractive workbench for testing any new computational or theoretical procedure.

In the present paper, we are interested in determining the energy spectrum of a two-electron quantum dot confined by a three-dimensional anisotropic harmonic potential without the application of an electromagnetic field. The spectrum, considering both singlet and triplet states, is computed using the discrete variable representation (DVR) method (see Refs. 78–80 and references therein). The DVR method, set with the Woods-Saxon potential, was recently used by us to study some confined quantum systems including one-electron quantum dot application.[37] We believe that this approach has the necessary flexibility and accuracy required by the low-dimensionality systems.

This paper is organized as follows. In Sec. II the theory of confined quantum dots is shown. Section III presents the discrete variable representation method in the fashion that we are using in calculations. The results are shown in Sec. IV. In Sec. V we present our concluding remarks.

II. THEORY

The Schrödinger equation for N confined particles is written as

$$H\Psi = E\Psi,\tag{1}$$

where

$$H(\mathbf{r}) = T(\mathbf{r}) + V_{\text{dot}}(\mathbf{r}) + V_{\text{int}}(\mathbf{r}),\tag{2}$$

with $\mathbf{r} \equiv \{\mathbf{r}_1, \mathbf{r}_2, \ldots, \mathbf{r}_N\}$ the position of N particles, T is the kinetic energy, V_{dot} is the confinement potential of the quantum dot, and V_{int} is the interaction potential between the particles.

The system of our interest is the two interacting electrons of effective mass m^* in a quantum dot with an anisotropic harmonic confinement potential whose Hamiltonian is

$$H = \sum_{j=1}^{2}\left\{-\frac{1}{2m^*}(\nabla_j^2) + V_{\text{dot}}(\mathbf{r}_j)\right\} + \frac{e^2}{\epsilon|\mathbf{r}_1 - \mathbf{r}_2|},\tag{3}$$

where ∇_j^2 is the Laplacian associated with the jth electron and

$$V_{\text{dot}}(\mathbf{r}_j) = \left(\frac{m^*}{2}\right)[\omega_\perp^2(x_j^2 + y_j^2) + \omega_z^2 z_j^2]\tag{4}$$

is the confinement potential of the quantum dot. The effective a.u. is used unless otherwise stated, i.e., $\hbar = m^* = e/\sqrt{\epsilon} = 1$.

The relative-motion ($\mathbf{r} = \mathbf{r}_1 - \mathbf{r}_2$) and center-of-mass ($\mathbf{R} = (\mathbf{r}_1 + \mathbf{r})/2$) coordinates in Eq. (3) can be introduced in order to split the Hamiltonian as follows:

$$H = H_{\text{CM}} + H_{\text{RM}},\tag{5}$$

where the center-of-mass (H_{CM}) term is

$$H_{\text{CM}} = -\frac{1}{4}\nabla_R^2 + \omega_\perp^2(X^2 + Y^2) + \omega_z^2 Z^2\tag{6}$$

and

$$H_{\text{RM}} = -\nabla_r^2 + \frac{1}{4}\omega_\perp^2(x^2 + y^2) + \frac{1}{4}\omega_z^2 z^2 + \frac{1}{r}\tag{7}$$

is the relative-motion (H_{RM}) term, with $r = |\mathbf{r}|$.

To solve Eq. (1) with the Hamiltonian expressed in Eq. (5), we can consider the spatial wave function of two-electron quantum dot as

$$\Psi = \phi_{\text{CM}}(\mathbf{R})\psi_{\text{RM}}(\mathbf{r}),\tag{8}$$

where $\phi_{\text{CM}}(\mathbf{R})$ and $\psi_{\text{RM}}(\mathbf{r})$ are solutions of the following equations:

$$H_{\text{CM}}\phi_{\text{CM}}(\mathbf{R}) = E_{\text{CM}}\phi_{\text{CM}}(\mathbf{R}),\tag{9}$$

$$H_{\text{RM}}\psi_{\text{RM}}(\mathbf{r}) = E_{\text{RM}}\psi_{\text{RM}}(\mathbf{r}).\tag{10}$$

Thus the total energy (E) of this system is the sum of the center-of-mass (E_{CM}) and relative-motion (E_{RM}) eigenenergies. From Eq. (9) the CM part can be solved analytically and its solution [$\phi_{\text{CM}}(\mathbf{R})$] is a planar oscillator with angular frequency $\omega_\perp$ and a Z-direction harmonic oscillator with frequency ω_z; in consequence, the CM eigenenergy can be written as

$$E_{\text{CM}} = (2N + |M| + 1)\omega_\perp + \left(N_Z + \frac{1}{2}\right)\omega_z,\tag{11}$$

where N and M are the radial and the azimuthal quantum numbers associated with the planar oscillator, respectively, and N_Z is the quantum number associated with the Z-direction harmonic oscillator.

The relative-motion problem defined in Eq. (10) has no analytical eigenfunction due to the Coulomb interaction. To solve it we have employed a variational scheme based on wave-function expansion in terms of a finite basis set. In particular, the DVR method[78] is used to expand $\psi_{\text{RM}}(\mathbf{r})$ in the radial direction, while the spherical harmonics are employed to expand it in the angular directions. The details of this procedure are described in the next section.

The total wave function (Ψ_{tot}) of the two-electron quantum dot should be defined as the product of spatial [$\Psi(\mathbf{R}, \mathbf{r})$] and spin parts, and it must be antisymmetric under the interchange of two electrons. This means that for singlet states the spatial wave function $\Psi(\mathbf{R}, \mathbf{r})$ must be symmetric, and for triplet states it must be antisymmetric. As the center-of-mass wave function [$\phi_{\text{CM}}(\mathbf{R})$] is always symmetric (the center-of-mass coordinate remains the same under the interchange of electrons), the symmetry condition should be in the relative motion described as [$\psi_{\text{RM}}(\mathbf{r})$]. It will be discussed later.

III. NUMERICAL PROCEDURE

The strategy to solve the relative-motion Schrödinger equation (10) is based on the variational principle where the problem is transformed into finding the stationary solutions of the functional $J[\psi_{RM}]$ given by

$$J[\psi_{RM}] = \int \psi_{RM}^*(\mathbf{r})(H_{RM} - E)\psi_{RM}(\mathbf{r})d\mathbf{r}. \tag{12}$$

As previously discussed, to obtain numerically the eigenvalues and eigenfunctions associated with Eq. (10), the relative motion wave function is first expanded in the following way,

$$\psi_{RM}^{\sigma m}(\mathbf{r}) = \sum_l \sum_j c_{lj}^{\sigma m} \frac{\chi_j(r)}{r} Y_{lm}(\Omega), \tag{13}$$

where $\{c_{lj}^{\sigma m}\}$ are the expansion coefficients, σ is the parity of the $\psi_{RM}(\mathbf{r})$ in relation to the interchange of the two electrons, and m is associated with the eigenvalue of the z component of the angular momentum operator l_z. Then, $J[\psi_{RM}]$ is required to be stationary under the variation of such coefficients. Next, the relative-motion problem turns out to be the solution of a generalized eigenvalue problem, which in matrix notation is the following equation:

$$\mathbf{H}_{RM}\mathbf{c}^{\sigma m} = E_{RM}^{\sigma m}\mathbf{S}\mathbf{c}^{\sigma m}, \tag{14}$$

where $\mathbf{c}^{\sigma m}$ is the coefficient vector. The Hamiltonian matrix elements are given by

$$\{\mathbf{H}_{RM}\}_{jj',ll'} = \int \chi_j^*(r)\left\{ -\frac{d^2}{dr^2} + \frac{l(l+1)}{r^2} + \frac{1}{4}\omega_\perp^2 r^2 + \frac{1}{r} \right\}$$
$$\times \chi_{j'}(r)dr\,\delta_{ll'} + \frac{\Delta\omega^2}{4}A_{l'}^{lm}\int \chi_j^*(r)r^2\chi_{j'}(r)dr, \tag{15}$$

with $\Delta\omega^2 = \omega_z^2 - \omega_\perp^2$ and

$$A_{l'}^{lm} = \int Y_{lm}^*(\Omega)\cos^2\theta Y_{l'm}(\Omega)d\Omega, \tag{16}$$

while

$$\{\mathbf{S}_{RM}\}_{jj',ll'} = \int \chi_j^*(r)\chi_{j'}(r)dr\,\delta_{ll'} \tag{17}$$

are the overlap matrix elements.

The symmetry condition of the $\psi_{RM}(\mathbf{r})$ should be done on the angular part of expansion (13) because r is symmetric under the interchange of electrons. As the parity of spherical harmonics is $(-1)^l$, expansion (13) can be separated into two: one with odd l's and the other with even l's. Thus, the total wave function Ψ_{tot} will be a singlet or a triplet state when the relative-motion wave function contains only odd l's or even l's in expansion (13), respectively. Moreover, as the z component of the angular momentum is conserved, the magnetic quantum number m is a good quantum number, and it is fixed during the calculation for each state. The other two quantum numbers, similar to the CM case, are one radial (n) associated with the planar motion and one (n_z) associated with the z-direction of the RM problem.

TABLE I. Intervals employed to solve Eq. (18) using the equally spaced DVR method for each couple of parameters $\omega_\perp$ and ω_z. Distances are in effective a.u.

$\omega_\perp$	ω_z	(a,b) interval
0.1	0.1	(0.0,35.0)
0.25	0.25	(0.0,25.0)
0.5	0.5	(0.0,20.0)
1.0	1.0	(0.0,15.0)
4.0	4.0	(0.0,10.0)
0.5	0.1	(0.0,40.0)
0.5	0.25	(0.0,25.0)
0.5	1.0	(0.0,20.0)
0.5	4.0	(0.0,20.0)

In the present work, the basis functions $\{\chi_j(r)\}$ are determined, solving the following eigenvalue problem:

$$\left[-\frac{d^2}{dr^2} + \frac{1}{4}\omega_\perp^2 r^2 + \frac{1}{r} \right]\chi_i(r) = \varepsilon_i\chi_i(r) \tag{18}$$

by using the equally spaced discrete variable representation method.[81–83] The DVR method is described with enough details in many other papers (e.g., see Refs. 78–80 and references therein). So, we will just introduce the method in what follows.

The DVR procedure consists of (i) building basis functions $\{f_i(r)\}$ with the property

$$f_i(r_j) = \frac{\delta_{ij}}{\sqrt{\omega_i}}, \quad i,j = 1,\ldots,k, \tag{19}$$

where $\{r_i\}$ and $\{\omega_i\}$ are the points and the weights of a Gaussian quadrature, (ii) expanding the trial wave function with the basis set (19),

$$\chi_i(r) = \sum_{j=1}^k d_{ji}f_j(r), \tag{20}$$

and (iii) solving the associated eigenvalue-eigenvector problem obtained from the variational principle. In such a method the matrix elements of the potential energy using the basis set (19) are diagonals,

$$\{\mathbf{V}\}_{ij} \approx V(r_i)\delta_{ij} = \left(\frac{1}{4}\omega_\perp^2 r_i^2 + \frac{1}{r_i} \right)\delta_{ij}, \tag{21}$$

while the kinetic-energy matrix elements $\{\mathbf{T}\}_{ij}$ should be, in general, determined analytically. Here the equally spaced DVR method is employed.[82] In this case, the $\{\mathbf{T}\}_{ij}$ can be then written as

$$\mathbf{T}_{ij} = \frac{(-1)^{i-j}}{(b-a)^2}$$
$$\times \frac{\pi^2}{2}\left\{ \frac{1}{\sin^2[\pi(i-j)/2N]} - \frac{1}{\sin^2[\pi(i+j)/2N]} \right\}, \quad i \neq j \tag{22}$$

and

TABLE II. Energy levels of the relative-motion problem [Eq. (14)] for the isotropic quantum dot as functions of (n,l), where n and l are the radial and angular momentum quantum numbers. Results are in effective a. u.

(n,l)	$E_{RM}(n,l)$				
	$\omega=0.1$	$\omega=0.25$	$\omega=0.5$	$\omega=1.0$	$\omega=4.0$
(0,0)	0.350 000	0.714 262	1.250 000	2.230 120	7.523 214
(0,1)	0.403 173	0.875 002	1.609 665	3.015 101	11.046 810
(0,2)	0.477 658	1.080 613	2.043 614	3.918 156	14.843 576
(1,0)	0.532 493	1.178 091	2.190 116	4.134 473	15.299 044
(0,3)	0.561 412	1.303 348	2.503 841	4.860 638	18.725 341
(1,1)	0.591 953	1.354 641	2.578 661	4.968 821	18.948 128
(0,4)	0.650 000	1.534 539	2.976 664	5.821 609	22.645 809
(1,2)	0.670 119	1.567 630	3.024 414	5.890 110	22.785 207
(2,0)	0.719 419	1.652 938	3.150 532	6.073 961	23.165 948
(0,5)	0.741 448	1.770 591	3.456 622	6.792 943	26.587 677
(1,3)	0.755 984	1.794 242	3.490 563	6.841 442	26.685 905
(2,1)	0.783 389	1.839 649	3.556 315	6.936 020	26.879 897
(0,6)	0.834 744	2.009 730	3.941 071	7.770 754	30.542 820
(1,4)	0.845 876	2.027 725	3.966 808	7.807 445	30.616 916
(2,2)	0.864 126	2.057 506	4.009 599	7.868 640	30.740 968
(3,0)	0.909 195	2.134 128	4.121 758	8.030 949	31.074 086
(0,7)	0.929 311	2.250 969	4.428 556	8.752 928	34.506 859
(1,5)	0.938 188	2.265 256	4.448 945	8.781 948	34.565 350
(2,3)	0.951 519	2.286 838	4.479 831	8.825 998	34.654 352
(3,1)	0.976 552	2.327 950	4.539 099	8.910 997	34.828 682
(0,8)	1.024 796	2.493 711	4.918 206	9.738 204	38.477 199
(1,6)	1.032 087	2.505 411	4.934 876	9.761 905	38.524 904
(2,4)	1.042 393	2.522 013	4.958 577	9.795 648	38.592 937
(3,2)	1.059 194	2.549 279	4.997 641	9.851 398	38.705 661
(4,0)	1.100 913	2.619 342	5.099 530	9.998 159	39.005 200
(0,9)	1.120 967	2.737 572	5.409 463	10.725 778	42.452 194
(1,7)	1.127 094	2.747 382	5.423 423	10.745 609	42.492 072
(2,5)	1.135 377	2.760 679	5.442 375	10.772 558	42.546 327
(3,3)	1.147 748	2.780 634	5.470 879	10.813 154	42.628 210
(4,1)	1.170 914	2.818 448	5.525 238	10.890 981	42.788 235
(0,10)	1.217 667	2.982 292	5.901 951	11.715 108	46.430 743
(1,8)	1.222 910	2.990 671	5.913 864	11.732 021	46.464 727
(2,6)	1.229 758	3.001 639	5.929 476	11.754 201	46.509 333
(3,4)	1.239 391	3.017 116	5.951 541	11.785 583	46.572 531
(4,2)	1.255 029	3.042 393	5.987 681	11.837 085	46.676 476
(5,0)	1.294 021	3.107 292	6.081 628	11.971 974	46.950 761
(0,11)	1.314 786	3.227 689	6.395 406	12.705 818	50.412 078
(1,9)	1.319 338	3.234 954	6.405 729	12.720 465	50.441 491
(2,7)	1.325 125	3.244 204	6.418 883	12.739 141	50.479 021
(3,5)	1.332 913	3.256 684	6.436 652	12.764 389	50.529 807
(4,3)	1.344 499	3.275 320	6.463 234	12.802 210	50.605 997
(5,1)	1.366 150	3.310 507	6.513 724	12.874 435	50.755 175

$$\mathbf{T}_{ii} = \frac{1}{(b-a)^2}\frac{\pi^2}{2}\left\{\frac{(2N^2+1)}{3} - \frac{1}{\sin^2[\pi(i)/N]}\right\}, \quad (23)$$

where $N=k+1$ and (a,b) are the intervals of integration.

A characteristic of the DVR method is that the value of an eigenfunction in a quadrature point is simply the coefficient of expansion (20) associated with the DVR function of this point divided by the root of the related weight,

$$\chi_i(r_j) = \frac{d_{ji}}{\sqrt{\omega_j}}. \quad (24)$$

It should be pointed out that the expressions in the DVR method depend only on the grid points; so, they are general

expressions for all one-dimensional systems. However, this procedure is easily extended to two-dimensional[83] and three-dimensional systems.[78]

IV. RESULTS

The energy spectra of the two-electron quantum dot confined by a three-dimensional anisotropic potential is determined for different parameters ($\omega_\perp$ and ω_z) by using the above procedure. The calculations are done expanding the wave function $\psi_{RM}(\mathbf{r})$ by using 30 spherical harmonics with a particular symmetry (odd or even l's) and 100 $\{\chi_i(r)\}$ basis functions. The solutions $\{\chi_i(r)\}$ of Eq. (18) are obtained employing 2500 DVR basis functions equally spaced in an ap-

TABLE III. Three-dimensional two-electron quantum dot energies for select values of the confinement parameter ω. Energies are in effective a.u.

ω	(N,L,n,l)	HF-1/N[a]	HF-num[b]	KS-1/N[c]	KS-num[d]	Exact-1/N[e]	Exact-num[f]	OIM[g]	DVR[h]
0.25	(0,0,0,0)	1.1163	1.1241	1.1644	1.1742	1.0858	1.08926		1.089 262
1.0	(0,0,0,0)	3.7673	3.7717	3.8711	3.8791	3.7217	3.73012	3.9632	3.730 120
	(0,0,0,1)							4.7167	4.515 101
	(0,0,0,2)							5.5867	5.418 156
	(0,0,0,3)							6.5075	6.360 638
	(0,0,0,4)							7.4532	7.321 609
4.0	(0,0,0,0)	13.5693	13.5693	13.7902	13.7928	13.5057	13.5232		13.523 214

[a]Hartree-Fock solutions by using the shifted 1/N method (Ref. 60).
[b]Hartree-Fock solutions by using the accurate numerical technique (Ref. 60).
[c]Kohn-Sham solutions by using the shifted 1/N method (Ref. 60).
[d]Kohn-Sham solutions by using the accurate numerical technique (Ref. 60).
[e]Exact Schrödinger solutions by using the shifted 1/N method (Ref. 60).
[f]Exact Schrödinger solutions by using the accurate numerical technique (Ref. 60).
[g]Exact Schrödinger solutions by using the orbital integration method (Ref. 59).
[h]Present results by using the discrete variable representation method.

propriate interval for each pair of parameters $\omega_\perp$ and ω_z. These intervals are shown in Table I. Thus, the energy spectra presented here have a good precision of at least six significant digits. In Sec. IV A the isotropic situation ($\omega_\perp = \omega_z$) is analyzed, while the anisotropic one ($\omega_\perp \neq \omega_z$) is shown in Sec. IV B.

A. Isotropic case

Initially the relative-motion eigenenergies (E_{RM}) are calculated by using the procedure described above for the following quantum dot parameters: $\omega_\perp = \omega_z \equiv \omega = 0.1$, 0.25, 0.5, 1.0, and 4.0. Due to the isotropy of the confinement potential, results can be labeled using n and l, the radial and angular momentum quantum numbers, respectively. This happens because the coupling term between different l's in Eq. (15) disappears due to $\Delta\omega = 0$ when $\omega_\perp = \omega_z$. Then, in such case, n and l are the quantum numbers associated with the relative-motion problem.

The first 42 relative-motion energy levels for each case are presented in Table II, where we can see some band structures in the results for larger values of ω. In each band, the n and l quantum numbers are related as follows: $2n + l = p$, p being an integer number. For example, the energy values of the states $(n,l) = (0,4)$, (1,2), and (2,0) are very close for $\omega = 1.0$ and 4.0, and they have $p = 4$. As we will point out later, this represents that the influence of the electron-electron interaction is smaller for the strong confinement than for the weak confinement.

On the other hand, to calculate the total energies (E) we do need to calculate the center-of-mass eigenenergies (E_{CM}). In the isotropic case, expression (11) is reduced to

$$E_{\mathrm{CM}} = \left(2N + L + \tfrac{3}{2}\right)\omega, \qquad (25)$$

where N and L denote, respectively, the radial and angular momentum quantum numbers related with the CM motion. Then, the complete spectrum ($E = E_{\mathrm{CM}} + E_{\mathrm{RM}}$) of the two-electron quantum dot confined by a three-dimensional isotropic harmonic potential can be determined from the results in Table II and Eq. (25). It is important to point out that RM and CM quantum states which are $2l + 1$ and $2L + 1$ degenerate with respect to the values of m and M, respectively.

The values of E for a small set of (N,L,n,l) states are presented in Table III in order to compare with the ones obtained previously in Refs. 59 and 60. These total energies of the two-electron quantum dot are determined in Ref. 60 solving the Hartree-Fock (HF), Kohn-Sham (KS), and Schrödinger (exact) equations by using the shifted, 1/N (1/N) (Ref. 84) and Schwartz numeric[85] (num) methods, while in Ref. 59 the ones are calculated by using the orbital integration method (OIM).[86] A comparison between the results shown in Table III indicates that the procedure based on the DVR method gives results with a great precision, and that the use of methodologies that compute completely the correlation effects is very important.
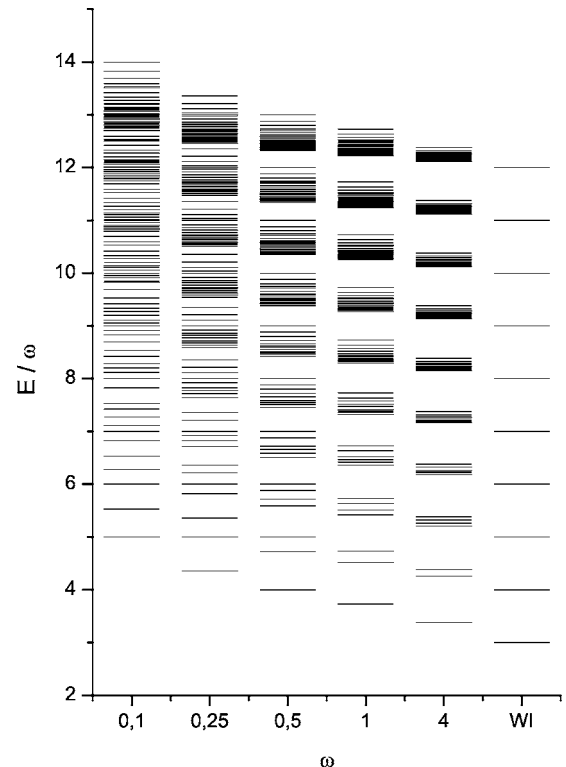

FIG. 1. Relative spectrum of isotropic two-electron quantum dot with respect to the confinement parameter ($E_{N,L,n,l}/\omega$) for five ω's (0.1, 0.25, 0.5, 1.0, and 4.0) and for the noninteracting (WI) case.
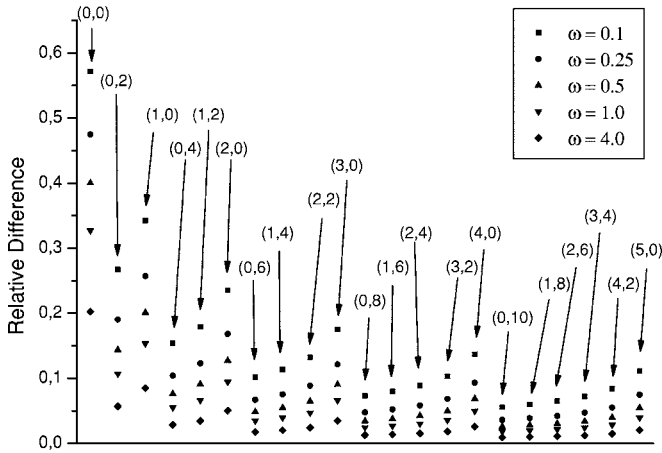
FIG. 2. Relative difference between the relative-motion singlet energy levels of the interacting and noninteracting isotropic two-electron quantum dot systems as a function of the (n,l) state for five different confinement parameters ($\omega=0.1$, 0.25, 0.5, 1.0, and 4.0)

Moreover, the spectrum with the lowest 245 energies of (N,L,n,l) states relative to the quantum dot parameter (i.e., E/ω) are displayed in Fig. 1 for five different ω's and for noninteracting electron problem (i.e., solutions of Eq. (3) where H_{RM} is written without the $1/r$ term). In the last case, relative-motion eigenenergies satisfy a similar expression of E_{CM} [Eq. (25)]; i.e., $E_{RM}=(2n+l+\frac{3}{2})\omega$. In this figure, the band structure appears clearly for $\omega \geqslant 0.5$, and when the values of the quantum dot parameter increase, the bands go sharpening and the interacting two-electron spectrum moves toward the noninteracting ones. However, for a weak confinement ($\omega \to 0$) it is observed that a spectrum diffuses more. Since the energy gaps that occur between the ($N+2L+n+2l+3$)-fold degenerate states of the noninteracting two-electron quantum dot (QD) is due to the spectrum associated with two harmonic oscillators, Fig. 1 indicates that for stronger QD parameters (larger values of ω) the motion of the electrons is mainly governed by the confinement potential, while for a weak confinement the electron-electron interaction plays an important and essential role.

In order to investigate this characteristic of the two-electron quantum dot, considered now are the relative-motion singlet states, i.e., solutions of Eq. (14) with odd values of the parameter l. For this purpose, in Fig. 2 are displayed the relative differences between the energy levels of the interacting and noninteracting systems [$\Delta E_{(n,l)}^{rel}=(E_{(n,l)}^{int}-E_{(n,l)}^{non})/E_{(n,l)}^{int}$] as a function of the (n,l) state. We can see in Fig. 2 that the error in the electron-electron interaction is clearly larger for the weak confinements than for the strong ones. For example, $\Delta E_{(0,0)}^{rel}$ for $\omega=0.1$ is approximately three times its value for $\omega=4.0$, while for $\Delta E_{(0,8)}^{rel}$ this difference is about six times. Another interesting aspect that can be pointed out is that the larger the angular quantum number l's, the smaller is the value of $\Delta E_{(n,l)}^{rel}$ when it is compared with the same band of energy levels. Moreover, the effect of the electron-electron interaction is larger in the low-lying states than in the highly excited ones. This issue can be explained if we call attention to the values of $\Delta E_{(0,l)}^{rel}$ and $\Delta E_{(n,0)}^{rel}$ when l and n are increased for all calculated ω's.
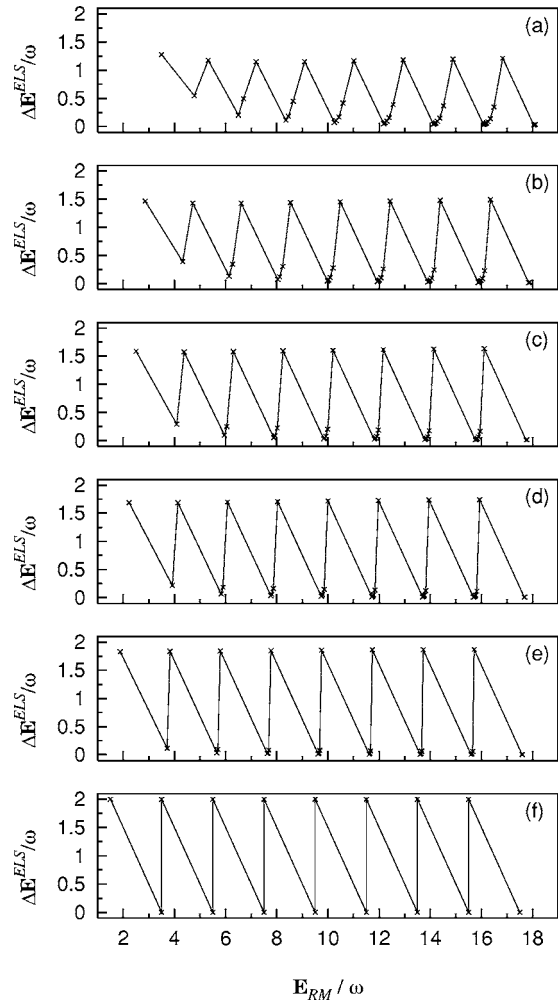

FIG. 3. Discrete relative-motion singlet energy-level spacing (ELS) for the isotropic two-electron quantum dot relative to ω as a function of relative energy for (a) $\omega=0.1$, (b) $\omega=0.25$, (c) $\omega=0.5$, (d) $\omega=1.0$, (e) $\omega=4.0$, and (f) noninteracting system.

The discrete energy-level spacing[55] (ELS) relative to ω [$\Delta E_i^{ELS}/\omega=(E_{i+1}-E_i)/\omega$] as a function of relative energy (E_i/ω) for singlets is shown in Fig. 3 for interacting systems with $\omega=0.1$, 0.25, 0.5, 0.1, and 4.0 for the noninteracting two-electron one. This figure supplies some information about the energy gaps that appear at the energy spectrum. The first is that energy gaps that occur in the noninteracting system are due to the spectrum of the harmonic oscillator. The second is that the energy gap decreases, and the degeneracies are lifted when the electron-electron interaction is included in the model. However, the intensities of these effects depend clearly on the quantum dot parameter ω. They are more obvious for the weak than for the strong confinement. Therefore, a repeated stretching phase of the energy gaps is observed for the interacting isotropic two-electron quantum dot. Note that a similar discussion was done for two-electron anisotropic two-dimensional quantum dots in Ref. 55.

B. Anisotropic case

The relative-motion eigenenergies (E_{RM}) associated with (n,m,n_z) states are calculated for the following quantum dot

TABLE IV. Energy levels of the relative-motion problem [Eq. (14)] for the anisotropic quantum dot for five ω_z parameters and $\omega_\perp=0.5$. The states are labeled by (n,m,n_z), where n and m are the radial and the azimuthal quantum numbers associated with the planar oscillator, respectively, and n_z is the quantum number associated with the z-direction harmonic oscillator. Results are in effective a.u.

$\omega_z=0.1$		$\omega_z=0.25$		$\omega_z=0.5$		$\omega_z=1.0$		$\omega_z=4.0$	
(0,0,0)	0.827 006	(0,0,0)	1.046 978	(0,0,0)	1.250 000	(0,0,0)	1.553 151	(0,0,0)	3.114 320
(0,0,1)	0.836 407	(0,0,1)	1.156 472	(0,1,0)	1.609 665	(0,1,0)	1.880 816	(0,1,0)	3.402 864
(0,0,2)	0.981 087	(0,0,2)	1.410 785	(0,0,1)	1.609 665	(0,2,0)	2.305 474	(0,2,0)	3.816 901
(0,0,3)	1.013 310	(0,1,0)	1.452 050	(0,2,0)	2.043 614	(1,0,0)	2.434 862	(1,0,0)	4.005 659
(0,0,4)	1.138 679	(0,0,3)	1.610 223	(0,1,1)	2.043 614	(0,0,1)	2.434 888	(0,3,0)	4.268 765
(0,0,5)	1.196 519	(0,1,1)	1.620 164	(0,0,2)	2.043 614	(0,1,1)	2.833 564	(1,1,0)	4.357 902
(0,1,0)	1.301 681	(0,0,4)	1.843 295	(1,0,0)	2.190 116	(1,1,0)	2.833 591	(0,4,0)	4.737 222
(0,0,6)	1.308 638	(0,1,2)	1.852 083	(0,3,0)	2.503 841	(0,4,0)	3.232 266	(1,2,0)	4.791 919
(0,1,1)	1.324 935	(0,2,0)	1.899 628	(0,2,1)	2.503 841	(1,2,0)	3.279 371	(2,0,0)	4.937 499
(0,0,7)	1.383 900	(1,0,0)	1.981 385	(0,1,0)	2.503 841	(0,2,1)	3.279 371	(0,5,0)	5.214 582
(0,1,2)	1.437 930	(0,0,5)	2.073 775	(0,0,3)	2.503 841	(2,0,0)	3.332 921	(1,3,0)	5.252 508
(0,0,8)	1.488 817	(0,1,3)	2.078 237	(1,1,0)	2.578 661	(1,0,1)	3.332 951	(2,1,0)	5.327 003
(0,1,3)	1.499 648	(0,2,1)	2.094 963	(1,0,1)	2.578 661	(0,0,2)	3.446 825	(0,6,0)	5.697 342
(0,0,9)	1.574 036	(1,0,1)	2.118 335	(0,4,0)	2.976 664	(0,5,0)	3.710 894	(1,4,0)	5.725 610
(0,1,4)	1.600 217	(0,0,6)	2.310 391	(0,3,1)	2.976 664	(0,3,1)	3.744 716	(2,2,0)	5.773 209
(0,0,10)	1.674 289	(0,1,4)	2.313 589	(0,2,2)	2.976 664	(1,3,0)	3.744 716	(3,0,0)	5.891 017
(0,1,5)	1.682 564	(0,2,2)	2.325 521	(0,1,3)	2.976 664	(1,1,1)	3.787 061	(0,7,0)	6.183 659
(0,0,11)	1.765 731	(0,3,0)	2.366 007	(0,0,4)	2.976 664	(2,1,0)	3.787 073	(1,5,0)	6.205 771
(0,2,0)	1.778 543	(1,0,2)	2.380 097	(1,2,0)	3.024 414	(0,1,2)	3.824 802	(2,3,0)	6.239 627
(0,1,6)	1.780 066	(1,1,0)	2.415 529	(1,1,1)	3.024 414	(0,6,0)	4.194 465	(3,1,0)	6.303 980
(1,0,0)	1.800 018	(0,0,7)	2.548 835	(1,0,2)	3.024 414	(1,4,0)	4.220 232	(0,8,0)	6.672 462
(0,2,1)	1.815 194	(0,1,5)	2.551 034	(2,0,0)	3.150 532	(0,4,1)	4.220 232	(1,6,0)	6.690 367
(1,0,1)	1.819 182	(0,2,3)	2.558 612	(0,5,0)	3.456 622	(2,2,0)	4.252 508	(2,4,0)	6.716 048
(0,0,12)	1.864 647	(0,3,1)	2.576 212	(0,4,1)	3.456 622	(1,2,1)	4.252 508	(3,2,0)	6.758 419
(0,1,7)	1.870 419	(1,0,3)	2.587 256	(0,3,2)	3.456 622	(0,2,2)	4.270 123	(4,0,0)	6.857 057
(0,2,2)	1.913 623	(1,1,1)	2.594 909	(0,2,3)	3.456 622	(3,0,0)	4.275 896	(0,0,1)	7.052 214
(1,0,2)	1.947 750	(0,0,8)	2.789 338	(0,1,4)	3.456 622	(2,0,1)	4.275 907	(0,9,0)	7.163 082
(0,0,13)	1.958 698	(0,1,6)	2.790 976	(0,0,5)	3.456 622	(1,0,2)	4.376 978	(1,7,0)	7.177 963
(0,1,8)	1.967 359	(0,2,4)	2.796 466	(1,3,0)	3.490 563	(0,0,3)	4.377 045	(2,5,0)	7.198 310
(0,2,3)	1.989 525	(0,3,2)	2.808 464	(1,2,1)	3.490 563	(0,7,0)	4.681 335	(3,3,0)	7.229 035
(1,0,3)	1.995 911	(1,0,4)	2.826 095	(1,1,2)	3.490 563	(1,5,0)	4.701 795	(4,1,0)	7.285 899
(0,0,14)	2.056 931	(1,1,2)	2.834 096	(1,0,3)	3.490 563	(0,5,1)	4.701 795	(0,1,1)	7.383 965
(0,1,9)	2.061 292	(0,4,0)	2.842 227	(2,1,0)	3.556 315	(1,3,1)	4.727 023	(0,10,0)	7.655 077
(0,2,4)	2.084 078	(1,2,0)	2.876 722	(2,0,1)	3.556 315	(2,3,0)	4.727 023	(1,8,0)	7.667 699
(1,0,4)	2.112 190	(2,0,0)	2.941 493	(0,6,0)	3.941 071	(0,3,2)	4.736 841	(2,6,0)	7.684 336
(0,0,15)	2.152 656	(0,0,9)	3.031 189	(0,5,1)	3.941 071	(2,1,1)	4.751 629	(3,4,0)	7.707 958
(0,1,10)	2.158 130	(0,1,7)	3.032 434	(0,4,2)	3.941 071	(3,1,0)	4.751 632	(4,2,0)	7.746 288
(0,2,5)	2.173 173	(0,2,5)	3.036 507	(0,3,3)	3.941 071	(0,1,3)	4.796 416	(0,2,1)	7.807 897
(1,0,5)	2.180 899	(0,3,3)	3.044 758	(0,2,4)	3.941 071	(1,1,2)	4.796 492	(5,0,0)	7.830 906
(0,0,16)	2.250 653	(1,0,5)	3.059 424	(0,1,5)	3.941 071	(0,8,0)	5.170 536	(1,0,1)	7.931 877
(0,1,11)	2.253 980	(0,4,1)	3.061 570	(0,0,6)	3.941 071	(1,6,0)	5.187 284	(1,9,0)	8.159 022
(0,3,0)	2.259 337	(1,1,3)	3.063 223	(1,4,0)	3.966 808			(2,7,0)	8.172 956

parameters: $\omega_z=0.1$, 0.25, 0.5, 1.0, and 4.0 with $\omega_\perp=0.5$. The first 42 relative-motion energy levels for each pair of ω_z and $\omega_\perp$ are presented in Table IV. They are also shown in Fig. 4 together with the noninteracting energy levels, which are given by $E_{RM}^{non}=(2n+m+1)\omega_\perp+(n_z+0.5)\omega_z$.

Some interesting information can be observed in Table IV and Fig. 4. The first one is the existence of a band structure in energy levels when the electron-electron interaction is considered, while to the noninteracting ones there is a regular structure. However, different from the isotropic case, the electronic states in these bands do not present a general rule. The second consideration is that the error obtained to calculate the noninteracting triplet ground state is smaller than the one obtained to calculate the noninteracting singlet ground

state. This indicates that the electron-electron interaction is more important for singlet states than for triplet ones. Similar conclusions were observed when we compare the results from Hartree-Fock and from the exact treatment for this system in Ref. 63. Moreover, some degeneracies between states with the same quantum number m but with different quantum numbers l and n_z can be seen for $\omega_z=1.0$ in Table IV. For example, the states $(0, m, 1)$ and $(1, m, 0)$ have the same energy within the results' precision.

In order to analyze the degeneracies that happen in the energy spectrum, the total-energy levels associated with (N,M,N_Z,n,m,n_z) states with up to two excitations for different ω_z's are shown in Table V. Some selected states from this table are displayed in Fig. 5 as functions of the ω_z pa-
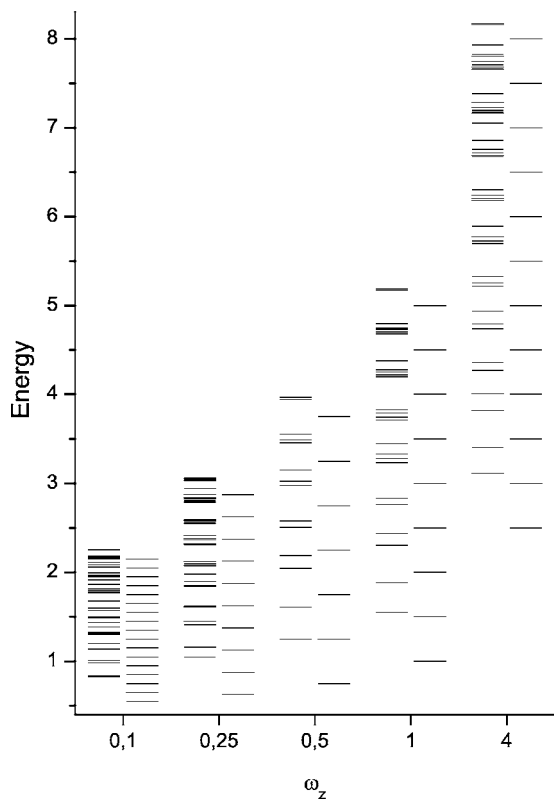
FIG. 4. Relative-motion energy levels of anisotropic two-electron quantum dot for ω_z=0.1, 0.25, 0.5, 1.0, and 4.0 with $\omega_\perp$=0.5. The first entry of each ω_z is associated with the interacting problem, while the second entry is related with the noninteracting one.

rameter. In such case the total energy is the addition of the relative-motion energy, shown in Table IV, with the center-of-mass energy given by Eq. (11). We can see a splitting on the degenerate total-energy levels for $\omega_\perp=\omega_z=0.5$ when ω_z varies. Moreover, other crossings of states happen for different ω_z's, as can be seen, for example, in Fig. 5 for ω_z=1.0 and for $\omega_z\approx0.38$. We can note that these crossings of energy levels are of two types: one is due to a symmetry of the confinement potential to particular ω parameters (as with ω_z=1.0), while the other is due to an accidental degeneracy which occurs between excited RM states and excited CM ones (as with $\omega_z\approx0.38$). The last one is the result of the electron-electron interaction and the vertical deformation. In a similar way it was pointed out by Sun and Ma in Ref. 41 during their studies of two-electron two-dimensional quantum dots confined by elliptical and bowl-like potentials. Besides, it can be seen also that the energy of an excited RM state, $(0, 0, 0, n, m, n_z)$, is always smaller than that of the similar excited CM state, $(N, M, N_Z, 0, 0, 0)$ with $N=n$, $M=m$, and $N_Z=n_z$. This can indicate that the effect of the electron-electron interaction is more accentuated, as the isotropic case, in the low-lying states than in the highly excited ones (remembering that the CM eigenenergy is equal to the RM one when the electron-electron interaction is taken off).

Figure 6 shows the ELS as a function of the relative-motion energy for singlets in interacting and noninteracting systems with different ω_z's. For $\omega_z \neq \omega_\perp$ the noninteracting ELS exhibits plateaus due to equidistant intracluster spacings that are not observed in the isotropic case. Some of these
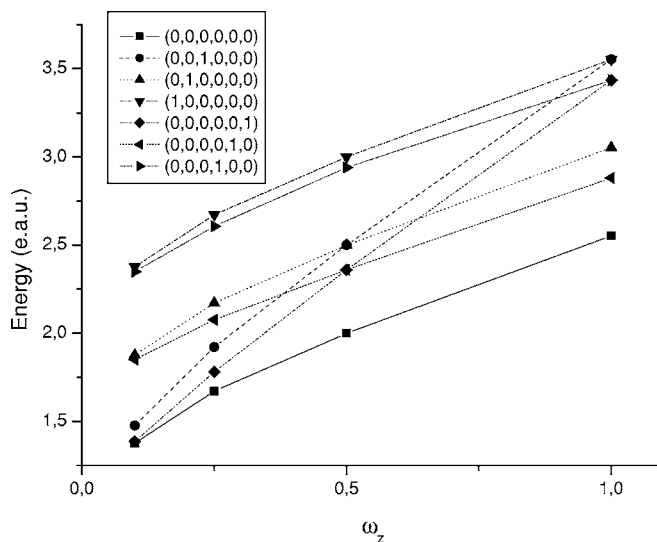

FIG. 5. Selected total-energy levels as a function of the ω_z parameter for the anisotropic two-electron quantum dot system with $\omega_\perp$=0.5.

plateaus remain when the electron-electron interaction as considered, for example, with ω_z=1.0, but some of them disappear with ω_z=4.0. It is interesting to note that the influence of the electron-electron interaction is greater for all calculations with different QD parameters ω_z's. However, here
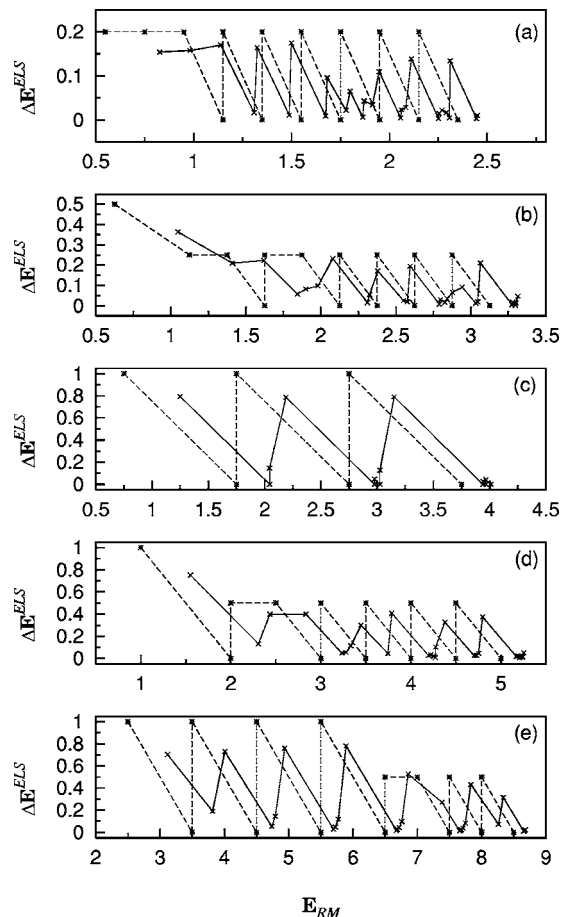

FIG. 6. Discrete relative-motion singlet energy-level spacing (ELS) as a function of relative-motion energy for interacting (full line) and noninteracting (dashed line) anisotropic two-electron quantum dots; (a) ω=0.1, (b) ω=0.25, (c) ω=0.5, (d) ω=1.0, and (e) ω=4.0.

TABLE V. Total-energy levels up to two excitations for the anisotropic two-electron quantum dot as functions of (N,M,N_z,n,m,n_z), where (N,M,N_z) are the quantum numbers associated with the CM problem and (n,m,n_z) are the quantum ones associated with the RM problem. Results are in effective a.u.

|	λ	$\omega_z=0.1$	$\omega_z=0.25$	$\omega_z=0.5$	$\omega_z=1.0$	$\omega_z=4.0$
a	(0,0,0,0,0,0)	(a) 1.377 006	(a) 1.671 978	(a) 2.000 000	(a) 2.553 151	(a) 5.614 320
b	(0,0,0,0,1,0)	(c) 1.386 407	(c) 1.781 472	(b) 2.359 665	(b) 2.880 816	(b) 5.902 864
c	(0,0,0,0,0,1)	(e) 1.477 006	(e) 1.921 978	(c) 2.359 665	(d) 3.053 151	(d) 6.114 320
d	(0,1,0,0,0,0)	(i) 1.486 407	(i) 2.031 472	(d) 2.500 000	(h) 3.305 474	(h) 6.316 901
e	(0,0,1,0,0,0)	(f) 1.531 087	(f) 2.035 785	(e) 2.500 000	(l) 3.380 816	(l) 6.402 864
f	(0,0,0,0,0,2)	(n) 1.577 006	(b) 2.077 050	(f) 2.793 614	(m) 3.434 862	(m) 6.505 659
g	(0,0,0,0,1,1)	(b) 1.851 681	(n) 2.171 978	(g) 2.793 614	(c) 3.434 888	(p) 6.614 320
h	(0,0,0,2,0,0)	(d) 1.877 006	(d) 2.171 978	(h) 2.793 614	(p) 3.553 151	(q) 6.614 320
i	(0,0,1,0,0,1)	(g) 1.874 935	(g) 2.245 164	(i) 2.859 665	(e) 3.553 151	(s) 6.857 902
j	(0,1,0,0,0,1)	(j) 1.886 407	(j) 2.281 472	(j) 2.859 665	(q) 3.553 151	(t) 6.902 864
k	(0,0,1,0,1,0)	(k) 1.951 681	(k) 2.327 050	(k) 2.859 665	(g) 3.833 564	(w) 7.005 659
l	(0,1,0,0,1,0)	(o) 1.977 006	(o) 2.421 978	(l) 2.859 665	(s) 3.833 591	(y) 7.114 320
m	(0,0,0,1,0,0)	(h) 2.328 543	(h) 2.524 628	(m) 2.940 116	(k) 3.880 816	(z) 7.437 499
n	(0,0,2,0,0,0)	(m) 2.350 018	(l) 2.577 050	(n) 3.000 000	(t) 3.880 816	(aa) 7.505 659
o	(0,1,1,0,0,0)	(l) 2.351 681	(m) 2.606 385	(o) 3.000 000	(w) 3.934 862	(ab) 7.614 320
p	(0,2,0,0,0,0)	(r) 2.369 182	(p) 2.671 978	(p) 3.000 000	(j) 3.934 888	(c) 9.552 214
q	(1,0,0,0,0,0)	(p) 2.377 006	(q) 2.671 978	(q) 3.000 000	(o) 4.053 151	(e) 9.614 320
r	(0,0,0,1,0,1)	(q) 2.377 006	(r) 2.743 335	(r) 3.328 661	(y) 4.053 151	(g) 9.883 965
s	(0,0,0,1,1,0)	(u) 2.386 407	(u) 2.781 472	(s) 3.328 661	(z) 4.332 921	(k) 9.902 864
t	(1,0,0,0,1,0)	(v) 2.450 018	(v) 2.856 385	(t) 3.359 665	(r) 4.332 951	(j)10.052 214
u	(1,0,0,0,0,1)	(x) 2.477 006	(x) 2.921 978	(u) 3.359 665	(aa) 4.434 862	(o)10.114 320
v	(0,0,1,1,0,0)	(s) 2.830 019	(s) 3.040 529	(v) 3.440 116	(v) 4.434 862	(r)10.431 877
w	(0,1,0,1,0,0)	(w) 2.850 018	(t) 3.077 050	(w) 3.440 116	(i) 4.434 888	(v)10.505 659
x	(1,0,1,0,0,0)	(t) 2.851 681	(w) 3.106 385	(x) 3.500 000	(u) 4.434 888	(u)10.552 214
y	(1,1,0,0,0,0)	(y) 2.877 006	(y) 3.171 978	(y) 3.500 000	(f) 4.446 825	(x)10.614 320
z	(0,0,0,2,0,0)	(z) 3.330 333	(z) 3.566 493	(z) 3.900 532	(n) 4.553 151	(f)13.527 801
aa	(1,0,0,1,0,0)	(aa) 3.350 018	(aa) 3.606 385	(aa) 3.940 116	(x) 4.553 151	(i)13.552 214
ab	(2,0,0,0,0,0)	(ab) 3.377 006	(ab) 3.671 978	(ab) 4.000 000	(ab) 4.553 151	(n)13.614 320
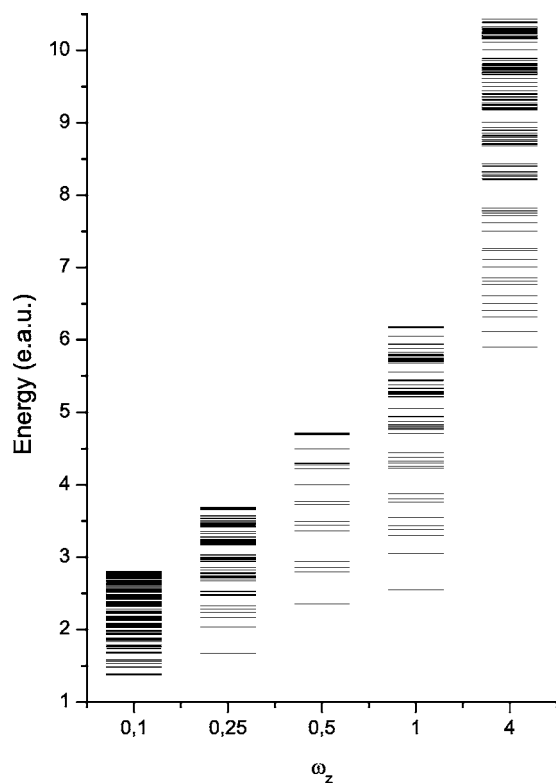
FIG. 7. Spectrum of anisotropic two-electron quantum dot for $\omega_z=0.1$, 0.25, 0.5, 1.0, and 4.0 with $\omega_\perp=0.5$.

are also observed behaviors that are similar to the isotropic situation. We can also note some energy gaps on the spectrum for noninteracting systems, and the reduction of the energy gaps and the break of the degeneracy when the interaction is considered in the model. This confirms the analysis in Ref. 55 for two-dimensional quantum dots that the electron-electron interaction changes the behavior of the ELS function significantly, and the preservation of this feature occurs only for the situation when it is compared with the noninteracting situation.

Finally, the spectrum of the two-electron anisotropic three-dimensional quantum dot to $\omega_z=0.1$, 0.25, 0.5, 1.0, and 4.0 with $\omega_\perp=0.5$ is displayed in Fig. 7. The band structures are observed for all ω's, but they appear more clearly for $\omega_z\geq0.5$. This indicates again that the motion of electrons is mainly governed by the confinement potential for strong QD parameters. In the anisotropic case, however, it cannot establish a general relation to the occurrence of degenerate states.

V. CONCLUSION

In this paper we have studied theoretically a two-electron quantum dot using a three-dimensional anisotropic harmonic confinement potential. In particular, we focus on the effect of the electron-electron interaction and the anisotropy on the ground and excited electronic states of the system. For this purpose, we have considered the isotropic (ω_1

$=\omega_z$) and anisotropic ($\omega_1 \neq \omega_z$) situations for different values of the QD parameters $\omega_\perp$ and ω_z. The spectra, considering both singlet and triplet states, have been computed using a variational approach based on the discrete variable representation method. The DVR method has been widely applied in literature to study problems in molecular and chemical physics, and here it is used with spherical harmonics, for the first time, to solve the eigenvalue-eigenvector equation of the relative motion of the electrons in a three-dimensional quantum dot. The procedure has shown very accurate calculations with at least six significant digits on the eigenvalues of energy. It is important to point out that the DVR method considers completely the electron-electron interaction.

The present results are displayed in Fig. 1–7 and Tables I–V. The major conclusions are summarized as follows: (i) The effects of the electron-electron interaction are more important for weak confinement potentials than for strong ones, for singlet states than for triplet states, and for low-lying states than for highly excited states. (ii) The degeneracies that exist in the noninteracting situation are lifted when the electron-electron interaction is included. (iii) The existence of vertical deformations breaking degeneracies that exist in the isotropic quantum dots. Other state crossings can appear for particular $\omega_\perp$ and ω_z parameters due to a combination of the electronic interaction and the vertical deformation. (iv) The observation of equidistant intracluster spacings of energy levels in quantum dots with anisotropic potential. And (v) the results obtained using the DVR method, when compared with others previously published, perform with great precision. So it demonstrates that such a method can be applied to the study of different confined quantum systems with confidence.

Finally, we call attention to the relation between values of the QD parameters ($\omega_\perp$ and ω_z) which defines the confinement intensity and the Coulombian interaction (see, for example, Fig. 1 for the isotropic case and Fig. 4 for the anisotropic situation). In this context it is interesting to note that a strong confinement is associated with a high-electronic density, while a weak confinement is associated with a low-electronic density. Moreover, we have verified that the electron-electron interaction is not so important for strong confinements; then in such a case the interaction can be treated as a perturbation of the noninteracting QD system. However, this is not true in the case of low-electronic density, and, in such a case, it is fundamental to employ or to develop methodologies which compute completely the electron-electron interaction like the one used in the present paper.

ACKNOWLEDGMENTS

[1] V. Fock, Z. Phys. **47**, 446 (1928).
[2] C. G. Darwin, Proc. Cambridge Philos. Soc. **27**, 86 (1930).
[3] A. Michels, J. de Boer, and A. Bijl, Physica (Amsterdam) **4**, 981 (1937).
[4] A. Sommerfeld and H. Welker, Ann. Phys. **32**, 56 (1938).
[5] E. Schrödinger, Proc. R. Ir. Acad., Sect. A **46**, 183 (1941).
[6] P. O. Fröman, S. Yngve, and N. Fröman, J. Math. Phys. **28**, 1813 (1987).
[7] W. Jaskólski, Phys. Rep. **271**, 1 (1996).
[8] J. P. Connerade, V. K. Dolmatov, and P. A. Laksbmit, J. Phys. B **33**, 251 (2000).
[9] L. Jacak, O. Hawrylak, and A. Wojs, *Quantum Dots* (Springer, New york 1998).
[10] A. Zrenner, J. Chem. Phys. **112**, 7790 (2000).
[11] R. C. Ashoori, Nature (London) **379**, 413 (1996).
[12] T. H. Dosterkamp, T. Fujisawa, W. G. van der Wiel, K. Ishibashi, R. V. Hijman, and L. P. Kouwenhoven, Nature (London) **395**, 823 (1998).
[13] N. F. Johnson, J. Phys.: Condens. Matter **7**, 965 (1995).
[14] S. Tarucha, D. G. Austing, T. Honda, R. T. van der Hage, and L. P. Kouwenhoven, Phys. Rev. Lett. **77**, 3613 (1996).
[15] K. H. Frank, R. Didde, H. J. Sagner, and W. Eberhardt, Phys. Rev. B **39**, 940 (1989).
[16] Z. K. Tang, Y. Nozue, and T. J. Goto, J. Phys. Soc. Jpn. **61**, 2943 (1992).
[17] H. W. Kroto, J. R. Heath, S. C. O'Brian, R. F. Curl, and R. E. Smalley, Nature (London) **318**, 162 (1985).
[18] I. Lazlo and L. Udvardi, Chem. Phys. Lett. **136**, 418 (1987).
[19] J. Cioslowski and E. D. Fleischmann, J. Chem. Phys. **94**, 3730 (1991).
[20] A. S. Baltenkov, J. Phys. B **32**, 2745 (1999).
[21] C. Reichardt, *Solvents and Solvents Effects in Organic Chemistry* (VCH, Weinheim, 1988).
[22] M. Takani, Comments At. Mol. Phys. **32**, 219 (1996).
[23] B. Saha, T. K. Mukherjee, P. K. Mukherjee, and G. H. F. Diercksen, Theor. Chem. Acc. **108**, 305 (2002).
[24] P. K. Mukherjee, J. Karwowski, and G. H. F. Diercksen, Chem. Phys. Lett. **363**, 323 (2002).
[25] M. Grinberg, W. Jaskólski, Cz. Koepke, J. Plannelles, and M. Janowicz, Phys. Rev. B **50**, 6504 (1994).
[26] V. Gudmundson and R. R. Gerhardts, Phys. Rev. B **43**, 12098 (1991).
[27] M. Grossmann and M. Holthaus, Z. Phys. B: Condens. Matter **97**, 319 (1995).
[28] J. H. Jefferson, M. Fearn, and D. L. J. Tipton, Phys. Rev. A **66**, 042328 (2002).
[29] G. Tóth and C. S. Lent, Phys. Rev. A **63**, 052315 (2001).
[30] P. L. Goodfriend, J. Phys. B **23**, 1373 (1990).
[31] Y. P. Varshni, J. Phys. B **30**, L589 (1997).
[32] R. Rivelino and J. D. M. Vianna, J. Phys. B **34**, L645 (2001).
[33] C. F. Destefani, J. D. M. Vianna, and G. E. Marques, Semicond. Sci. Technol. **19**, L90 (2004).
[34] M. N. Guimarães and F. V. Prudente, J. Phys. B **38**, 2811 (2005).
[35] C. Zicovich-Wilson, J. H. Planelles, and W. Jaskólski, Int. J. Quantum Chem. **50**, 429 (1994).
[36] E. Ley-Koo and S. Rubinstein, J. Chem. Phys. **71**, 351 (1979).
[37] L. S. Costa, F. V. Prudente, P. H. Acioli, J. J. Soares Neto, and J. D. M. Vianna, J. Phys. B **32**, 2461 (1999).
[38] U. Merkt, J. Huser, and M. Wagner, Phys. Rev. B **43**, 7320 (1991).
[39] M. Macucci, K. Hess, and G. J. Iafrate, Phys. Rev. B **48**, R4879 (1997).
[40] C. Yannouleas and U. Landman, Phys. Rev. Lett. **85**, 1726 (2000).
[41] L. L. Sun and F. C. Ma, J. Appl. Phys. **94**, 5844 (2003).
[42] S. Bednarek, B. Szafran, and J. Adamowski, Phys. Rev. B **59**, 13036 (1999).
[43] D. C. Thompson and A. Alavi, Phys. Rev. B **66**, 235118 (2002).
[44] J. Jung and J. E. Alvarellos, J. Chem. Phys. **118**, 10825 (2003).
[45] J. Jung, P. García-González, J. E. Alvarellos, and R. W. Godby, Phys. Rev. A **69**, 052501 (2004).
[46] D. C. Thompson and A. Alavi, J. Chem. Phys. **122**, 124107 (2005).
[47] D. Pfannkuche and R. R. Gerhardts, Phys. Rev. B **44**, 13132 (1991).
[48] E. A. Salter, G. W. Trucks, and D. S. Cyphert, Am. J. Phys. **69**, 120 (2001).
[49] G. W. Bryant, Phys. Rev. Lett. **59**, 1140 (1987).
[50] E. Räsänen, A. Harju, M. J. Puska, and R. M. Nieminen, Phys. Rev. B **69**, 165309 (2004).
[51] A. Alavi, J. Chem. Phys. **113**, 7735 (2000).
[52] D. M. Mitnik, Phys. Rev. A **70**, 022703 (2004).
[53] G. Cantele, D. Ninno, and G. Iadonisi, Phys. Rev. B **64**, 125325 (2001).
[54] J. Adamowski, M. Sobkowicz, B. Szafran, and S. Bednarek, Phys. Rev. B **62**, 4234 (2000).
[55] P. S. Drouvelis, P. Schmelcher, and F. K. Diakonos, Phys. Rev. B **69**, 035333 (2004).
[56] N. R. Kestner and O. Sinanoglu, Phys. Rev. **128**, 2687 (1962).
[57] J. Cioslowski and K. Pernal, J. Chem. Phys. **113**, 8434 (2000).

[58] P. M. Laufer and J. B. Krieger, Phys. Rev. A **33**, 1480 (1986).
[59] W. C. Lee and T. K. Lee, J. Phys.: Condens. Matter **14**, 1045 (2002).
[60] R. Pino and V. M. Villalba, J. Phys.: Condens. Matter **13**, 11651 (2001).
[61] T. Sako and G. H. F. Diercksen, J. Phys.: Condens. Matter **15**, 5487 (2003).
[62] J. T. Lin and T. F. Jiang, Phys. Rev. B **64**, 195323 (2001).
[63] D. Pfannkuche, V. Gudmundsson, and P. A. Maksym, Phys. Rev. B **47**, 2244 (1993).
[64] C. E. Creffield, J. H. Jefferson, S. Sarkar, and D. L. J. Tipton, Phys. Rev. B **62**, 7249 (2000).
[65] S. Kais, D. R. Herschbach, N. C. Handy, C. W. Murray, and G. J. Laming, J. Chem. Phys. **99**, 417 (1993).
[66] B. Szafran, S. Bednarek, J. Adamowski, M. B. Tavernier, E. Anisimovas, and F. M. Peeters, Eur. Phys. J. D **28**, 373 (2004).
[67] T. F. Jiang, X. Tong, and S. Chu, Phys. Rev. B **63**, 045317 (2001).
[68] M. Wagner, U. Merkt, and A. V. Chaplik, Phys. Rev. B **45**, 1951 (1992).
[69] G. Cipriani, M. Rosa-Clot, and S. Taddei, Phys. Rev. B **61**, 7536 (2000).
[70] A. Harju, V. A. Sverdlov, R. M. Nieminen, and V. Halonen, Phys. Rev. B **59**, 5622 (1999).
[71] J. Harting, O. Mülken, and P. Borrmann, Phys. Rev. B **62**, 10207 (2000).
[72] M. Taut, Phys. Rev. A **48**, 3561 (1993).
[73] M. Dineykhan and R. G. Nazmitdinov, Phys. Rev. B **55**, 13707 (1997).

[74] S. Kais, D. R. Herschbach, and R. D. Levine, J. Chem. Phys. **91**, 7791 (1989).
[75] S. Klama and E. G. Mishchenko, J. Phys.: Condens. Matter **10**, 3411 (1998).
[76] L. Serra, R. G. Nazmitdinov, and A. Puente, Phys. Rev. B **68**, 035341 (2003).
[77] T. Sako and G. H. F. Diercksen, J. Phys. B **36**, 1681 (2003).
[78] J. C. Light and T. Carrington, Jr., Adv. Chem. Phys. **114**, 263 (2000).
[79] F. V. Prudente, A. Riganelli, and A. J. C. Varandas, Rev. Mex. Fis. **47**, 568 (2001).
[80] R. G. Littlejohn, M. Cargo, T. Carrington, Jr., K. A. Mitchell, and B. Poirier, J. Chem. Phys. **116**, 8691 (2002).
[81] J. T. Muckerman, Chem. Phys. Lett. **173**, 200 (1990).
[82] D. T. Colbert and W. H. Miller, J. Chem. Phys. **96**, 1982 (1992).
[83] F. V. Prudente, L. S. Costa, and J. J. Soares Neto, J. Mol. Struct.: THEOCHEM **394**, 169 (1997).
[84] T. Imbo, A. Pagnamenta, and U. Sukhatme, Phys. Rev. D **29**, 1669 (1984).
[85] C. Schwartz, J. Math. Phys. **26**, 411 (1985).
[86] R. Friedberg, T. D. Lee, and W. Q. Zhao, Nuovo Cimento Soc. Ital. Fis., A **112A**, 1195 (1999).